

AD-A072 396

NAVAL RESEARCH LAB WASHINGTON DC

F/G 20/9

THE OSCILLATING TWO STREAM AND PARAMETRIC DECAY INSTABILITIES I--ETC(U)

JUL 79 H P FREUND, K PAPADOPOULOS

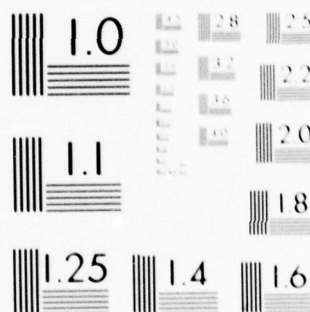
UNCLASSIFIED

NRL-MR-4042


NL

| OF |
AD
A072396





MICROCOPY RESOLUTION TEST CHART
NATIONAL BUREAU OF STANDARDS-1963-A

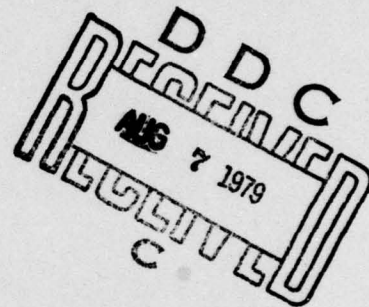
 NRL Memorandum Report 4042

**The Oscillating Two Stream and Parametric Decay
Instabilities in a Weakly Magnetized Plasma**

H. P. FREUND AND K. PAPADOPOULOS

Plasma Physics Division

LEVEL



July 23, 1979



NAVAL RESEARCH LABORATORY
Washington, D.C.

Approved for public release; distribution unlimited.

79 08 03 043

AD A 072396

DDC FILE COPY

SECURITY CLASSIFICATION OF THIS PAGE (When Data Entered)

REPORT DOCUMENTATION PAGE		READ INSTRUCTIONS BEFORE COMPLETING FORM
1. REPORT NUMBER NRL Memorandum Report 4042	2. GOVT ACCESSION NO.	3. RECIPIENT'S CATALOG NUMBER
4. TITLE (and Subtitle) THE OSCILLATING TWO STREAM AND PARAMETRIC DECAY INSTABILITIES IN A WEAKLY MAGNETIZED PLASMA	5. TYPE OF REPORT & PERIOD COVERED Interim report on a continuing NPL problem.	
7. AUTHOR(s) H. P. Freund and K. Papadopoulos	8. CONTRACT OR GRANT NUMBER(s) 12 33p	
9. PERFORMING ORGANIZATION NAME AND ADDRESS Naval Research Laboratory Washington, DC 20375	10. PROGRAM ELEMENT, PROJECT, TASK AREA & WORK UNIT NUMBERS Project W-14, 365 NRL Problem A03-31	
11. CONTROLLING OFFICE NAME AND ADDRESS National Aeronautics & Space Administration Hq. Contracts Division, Code JHC-3 Washington, DC 20546	12. REPORT DATE July 22 1979	
14. MONITORING AGENCY NAME & ADDRESS (if different from Controlling Office)	13. NUMBER OF PAGES 32	
	15. SECURITY CLASS. (of this report) UNCLASSIFIED	
	16. DECLASSIFICATION/DOWNGRADING SCHEDULE	
16. DISTRIBUTION STATEMENT (of this Report) Approved for public release; distribution unlimited. 14 NRL-MR-4042		
17. DISTRIBUTION STATEMENT (of the abstract entered in Block 20, if different from Report)		
18. SUPPLEMENTARY NOTES This Research was sponsored by NASA Project No. W-14,365.		
19. KEY WORDS (Continue on reverse side if necessary and identify by block number) Parametric instabilities Oscillating two stream instability Parametric decay instability Modulational instabilities.		
20. ABSTRACT (Continue on reverse side if necessary and identify by block number) We consider the effects of a weak ambient magnetic field on the oscillating two stream and parametric decay instabilities, with particular emphasis on the dependence on the angular variation of the instability thresholds and growth rates on the magnetic field. A dispersion relation is derived in the limit in which $\omega \gg \Omega_e$ (where ω and Ω_e are the electron plasma and cyclotron frequencies respectively), and is solved for dipole and monochromatic pump spectra. The analysis shows that the presence of a magnetic field can substantially enhance thresholds and reduce growth rates for (Continues)		

DD FORM 1 JAN 73 1473

EDITION OF 1 NOV 65 IS OBSOLETE
S/N 0102-014-6601

SECURITY CLASSIFICATION OF THIS PAGE (When Data Entered)

251950 LHM

20. Abstract (Continued)

waves propagating at an oblique angle with respect to the magnetic field and $k^2 \lambda_e^2 \sim \Omega_e^2 / \omega_e^2$ (where k is the wavevector of the perturbation and λ_e the Debye length). Thus, the magnetic field has a stabilizing influence on the off-parallel propagating modes.

$\lambda_{\text{sub } e}$

$$(k \lambda_{\text{sub } e})^2 \text{ - squared approximately } =$$

$$(\Omega_{\text{sub } e} / \omega_{\text{sub } e})^2 \text{ - squared}$$

CONTENTS

I. INTRODUCTION	1
II. THE BASIC EQUATIONS	3
III. THE DISPERSION EQUATION	8
A. The Dipole Approximation	10
B. The Case of a Monochromatic Pump	12
IV. SUMMARY AND DISCUSSION	16
ACKNOWLEDGMENTS	18
REFERENCES	19

Accession For	
NTIS GRA&I	<input checked="" type="checkbox"/>
DDC TAB	<input type="checkbox"/>
Unannounced	<input type="checkbox"/>
Justification	<input type="checkbox"/>
By _____	
Distribution/	
Availability Codes	
Dist	Avail and/or special
A	

I. INTRODUCTION

A great deal of attention has been focussed on the study of parametric processes in plasmas because of their importance to both laser- and beam-plasma interactions, as well as to anomalous heating mechanisms. The thrust behind the present work is directed towards an understanding of the parametric stabilization of beam-plasma interactions. In all such processes, the underlying concept is a three wave interaction in which a large amplitude pump wave (ω_0, k_0) excites two new waves (ω_1, k_1) and (ω_2, k_2) subject to the requirements that $\omega_0 = \omega_1 \pm \omega_2$ and $k_0 = k_1 \pm k_2$. In the case of beam-plasma systems, stabilization can occur due to the nonlinear transfer of energy away from beam resonant modes via a parametric coupling of high and low frequency waves. Recent work in this regard¹⁻⁵ has dealt largely with unmagnetized systems, in which a wave-particle resonance is possible only for longitudinal electron plasma oscillations. Nonlinear coupling proceeds, therefore, between high frequency Langmuir and low frequency ion acoustic waves, and may be treated within the context of the electrostatic approximation.

The instability which arises from the interaction of a large amplitude Langmuir pump wave and secondary (or daughter) Langmuir and ion acoustic waves has been extensively studied in the literature⁶⁻⁹ in a field-free plasma, for which two fundamental regimes of interest are found. One case occurs for $\omega_0 > \omega_1$ and $|k_0| > |k_1|$ (where we use ω_1, k_1 to denote the secondary Langmuir wave), and is referred to as the parametric decay instability. In the opposite case in which $\omega_0 < \omega_1$ and $|k_0| < |k_1|$, the oscillating two stream instability is obtained. We

Note: Manuscript submitted May 17, 1979.

observe that the phase velocity of the secondary Langmuir wave is greater (less) than that of the pump wave for the parametric decay (oscillating two stream) instability.

It is our purpose in this work to study the effect of weak magnetic fields upon the oscillating two stream and parametric decay instabilities. In particular, we are concerned with the effect of the magnetic field on the angular variation in the instability thresholds and growth rates. Direct application of the work is primarily to the physics of electron streams in the solar wind, and on type III solar bursts^{1,3} in particular. In addition, since the equations governing the oscillating two stream and parametric decay instabilities are the Fourier transforms of the equations governing Langmuir solitons, the work has implications on the characteristics of Langmuir solitons in a weakly magnetized plasma.

The organization of the paper is as follows. In Sec. II, we define the physical configuration to be employed and derive the basic equations governing the nonlinear coupling between Langmuir and ion acoustic waves. These equations are solved in Sec. III for both a dipole and monochromatic pump spectrum, and a numerical analysis is presented. A summary and discussion is given in Sec. IV.

II. THE BASIC EQUATIONS

The fundamental equations which describe the dynamical behavior of the system are generalizations of Zakharov's equations for Langmuir solitons¹⁰ to a physical configuration which includes a uniform ambient magnetic field $B_0 (\equiv B_0 \hat{e}_z)$. We write the ion and electron density in the form $n_i = n_0 + \delta n$ and $n_e = n_0 + \delta n + \delta n_e$ where n_0 is the ambient density, δn denotes the low frequency fluctuation in the ion and electron densities, and δn_e is the high frequency component of the electron density perturbation. In addition, we assume that there is no bulk flow of either electrons or ions, and employ δu_i and δu_e to describe the slow perturbations in the ion and electron velocities, and δv_e to describe the fast electron velocity fluctuations. Finally, E and δE are used to denote the low and high frequency components of the electric field perturbations.

First consider the equations which describe the high frequency oscillations. In this case, the electron continuity and momentum transfer equations, as well as Poisson's equations, can be written to lowest order as

$$\frac{\partial}{\partial t} \delta n_e + n_0 \left(1 + \frac{\delta n}{n_0} \right) \nabla \cdot \delta \chi_e = 0, \quad (1)$$

$$\frac{\partial}{\partial t} \delta \chi_e = - \frac{e}{m_e} \delta E - \frac{3v_e^2}{m_e} \left(1 + \frac{\delta n}{n_0} \right)^{-1} \nabla \delta n_e - \Omega_e (\delta \chi_e \times \hat{e}_z), \quad (2)$$

$$\nabla \cdot \delta E = - 4\pi e \delta n_e, \quad (3)$$

where $v_e \equiv (T_e/m_e)^{1/2}$ denotes the electron thermal speed, and $\Omega_e \equiv |eB_0/m_e c|$. It should be noted here that second order terms in δn_e and $\delta \chi_e$ have been neglected in (1) and (2). Elimination of δn_e and $\delta \chi_e$ from (1) - (3) yields, after some manipulation, the following result

$$\begin{aligned} \nabla \cdot \left(\frac{\partial^2}{\partial t^2} \left[\frac{\partial^2}{\partial t^2} + \omega_e^2 \left(1 + \frac{\delta n}{n_0} \right) - 3\omega_e^2 \lambda_e^2 \nabla^2 + \Omega_e^2 \right] - 3\omega_e^2 \Omega_e^2 \lambda_e^2 \nabla_{\parallel}^2 \right) \delta E = \\ = - \omega_e^2 \Omega_e^2 \left(1 + \frac{\delta n}{n_0} \right) \nabla_{\parallel} \cdot \delta E, \end{aligned} \quad (4)$$

where $\omega_e^2 \equiv 4\pi e^2 n_0 / m_e$, $\lambda_e \equiv v_e / \omega_e$, and $\nabla_{\parallel} \equiv \hat{e}_z (\hat{e}_z \cdot \nabla)$. If we note that $\nabla^2 \nabla_{\parallel} \cdot \delta E = \nabla_{\parallel}^2 \nabla \cdot \delta E$, then it is clear that

$$\begin{aligned} \left(\frac{\partial^2}{\partial t^2} \nabla^2 \left[\frac{\partial^2}{\partial t^2} + \omega_e^2 (1 - 3\lambda_e^2 \nabla^2) + \Omega_e^2 \right] + \omega_e^2 \Omega_e^2 \nabla_{\parallel}^2 (1 - 3\lambda_e^2 \nabla^2) \right) \delta E = \\ = - \omega_e^2 \left(\nabla^2 \frac{\partial^2}{\partial t^2} + \Omega_e^2 \nabla_{\parallel}^2 \right) \frac{\delta n}{n_0} \delta E. \end{aligned} \quad (5)$$

After Fourier transformation in space, (5) becomes

$$\begin{aligned} \left(\frac{\partial^4}{\partial t^4} + (\omega_k^2 + \Omega_e^2) \frac{\partial^2}{\partial t^2} + \frac{k_{\parallel}^2}{k^2} \omega_k^2 \Omega_e^2 \right) \delta E(k, t) = \\ = - \omega_e^2 \left(\frac{\partial^2}{\partial t^2} + \frac{k_{\parallel}^2}{k^2} \Omega_e^2 \right) \int d^3 k' \frac{\delta n(k-k', t)}{n_0} \delta E(k', t), \end{aligned} \quad (6)$$

where $\omega_k^2 \equiv \omega_e^2 (1 + 3k^2 \lambda_e^2)$, $\delta E(k, t)$ and $\delta n(k, t)$ are the spatial Fourier amplitudes associated with the wavevector k , and $k_{\parallel} \equiv k \cdot \hat{e}_z$.

The fourth order linear differential operator on the left-hand-side of (6) can be written as the product of two second order differential operators $(\partial^2/\partial t^2 + \omega_1^2) (\partial^2/\partial t^2 + \omega_2^2)$, where

$$\omega_{1,2}^2 = \frac{1}{2}(\omega_k^2 + \Omega_e^2) \pm \frac{1}{2} \left[(\omega_k^2 + \Omega_e^2)^2 - 4 \frac{k_{\parallel}^2}{k^2} \omega_k^2 \Omega_e^2 \right]^{1/2}, \quad (7)$$

and reduces to the usual cold plasma resonance frequencies in the limit $T_e \rightarrow 0$. Substantial simplification occurs only in the limit in which $\Omega_e^2 \ll \omega_e^2 \leq \omega_k^2$, where (for $k_{\perp}^2 \equiv k^2 - k_{\parallel}^2$) $\omega_1^2 \approx \omega_k^2 + (k_{\perp}^2/k^2) \Omega_e^2$ and $\omega_2^2 \approx (k_{\parallel}^2/k^2) \Omega_e^2$ correct to within terms of order $(\Omega_e/\omega_e)^4$. In this regime, Eq. (6) can be written in the comparatively simple form

$$\left(\frac{\partial^2}{\partial t^2} + \omega_k^2 + \frac{k_{\perp}^2}{k^2} \Omega_e^2 \right) \delta E(k, t) = - \frac{\omega_e^2}{n_0} \int d^3 k' \delta n(k - k', t) \delta E(k', t). \quad (8)$$

Finally, if it is assumed that $\delta E(k, t) = \text{Re} [\delta \mathcal{E}(k, t) \exp(-i\omega_e t)]$, where $k \delta \mathcal{E}(k, t) = k_{\parallel} \delta \epsilon(k, t)$ and $|(\partial/\partial t) \delta \epsilon(k, t)| \ll \omega_e |\delta \epsilon(k, t)|$, then it follows that

$$\left(i \frac{\partial}{\partial t} - \frac{3}{2} \omega_e (k \lambda_e)^2 - \frac{1}{2} \frac{k_{\perp}^2}{k^2} \frac{\Omega_e^2}{\omega_e} \right) \delta \epsilon(k, t) = \frac{\omega_e}{2n_0} \int d^3 k' \left(\frac{k \cdot k'}{k k'} \right) \times \delta n(k - k', t) \delta \epsilon(k', t) \quad (9)$$

for $(k \lambda_e)^2 \ll 1$.

In the treatment of the slow frequency ion oscillations we assume that the wave frequency is much greater than the ion gyrofrequency and the wavelength is much less than the ion Larmor radius. In such a regime the ions are effectively unmagnetized, and we write the ion continuity and momentum transfer equations

$$\frac{\partial}{\partial t} \delta n + n_0 \nabla \cdot \delta \mathbf{u}_i = 0, \quad (10)$$

$$n_0 m_i \frac{\partial}{\partial t} \delta \mathbf{u}_i = en_0 \mathbf{E} - \nabla \phi_i - \gamma_i T_i \nabla \delta n. \quad (11)$$

If it is assumed, in addition, that the wave frequency $\omega \ll k_{\parallel} v_e$, then the low frequency electron response can be described by

$$0 = -en_0 \mathbf{E} - \nabla \phi_e - \gamma_e T_e \nabla \delta n, \quad (12)$$

where the electron inertia has been neglected. In (11) and (12),

ϕ_α , γ_α , and T_α ($\alpha = i, e$) are the ion and electron ponderomotive potentials, ratio of specific heats, and temperatures respectively.

Combination of (11) and (12) immediately yields

$$\left(\frac{\partial^2}{\partial t^2} - c_s^2 \nabla^2 \right) \delta n = \frac{1}{m_i} \nabla^2 (\phi_i + \phi_e), \quad (13)$$

where $c_s^2 \equiv (\gamma_i T_i + \gamma_e T_e)/m_i$ is the acoustic velocity. It can be shown^{11,12} that the ponderomotive potentials are given by

$\phi_e = (m_i/m_e) \phi_i = \delta \mathcal{E}^2 / 8\pi$ correct to within terms of order $(\Omega_e/\omega_e)^2$ and $\lambda_e^2 |\nabla \nabla \cdot \delta \mathcal{E}| / |\delta \mathcal{E}|$. As a result, we may write that

$$\begin{aligned} \left(\frac{\partial^2}{\partial t^2} + k^2 c_s^2 \right) \delta n(\mathbf{k}, t) = & - \frac{k^2}{16\pi m_i} \int d^3 k' \frac{(\mathbf{k} - \mathbf{k}') \cdot \mathbf{k}'}{k' |\mathbf{k} - \mathbf{k}'|} \delta \epsilon^*(\mathbf{k} - \mathbf{k}', t) \\ & \times \delta \epsilon(\mathbf{k}', t) + O\left(\frac{\Omega_e^2}{\omega_e^2}, k^2 \lambda_e^2\right). \end{aligned} \quad (14)$$

Equations (9) and (14) constitute a pair of coupled nonlinear equations for the high and low frequency perturbations. In order to linearize these equations we assume that $\delta\epsilon(k, t) = \epsilon_0(k, t) + \delta\epsilon_1(k, t)$, where $\delta\epsilon_0$ and $\delta\epsilon_1$ represent Langmuir pump and daughter waves respectively and it is assumed that $\delta\epsilon_1$ is a small perturbation. The pump spectrum is taken to have a width Δk_0 centered about k_0 , and for sufficiently small Δk_0 we obtain

$$\left(i \frac{\partial}{\partial t} - \frac{3}{2} \omega_e (k \lambda_e)^2 - \frac{1}{2} \frac{k^2}{k^2} \frac{\Omega_e^2}{\omega_e} \right) \delta\epsilon_1(k, t) = \frac{\omega_e}{2n_0} \int d^3k' \left(\frac{k \cdot k'}{k k'} \right) \times \delta n(k - k', t) \epsilon_0(k', t), \quad (15)$$

and

$$\left(\frac{\partial^2}{\partial t^2} + k^2 c_s^2 \right) \delta n(k, t) = - \frac{k^2}{16\pi n_1} \int d^3k' \frac{(k - k') \cdot k'}{k' |k - k'|} \left(\epsilon_0(k', t) \delta\epsilon_1^*(k - k', t) + \epsilon_0^*(k - k', t) \delta\epsilon_1(k', t) \right). \quad (16)$$

III. THE DISPERSION EQUATION

The dispersion equation may be obtained from Eqs. (15) and (16) by means of Green's function techniques, and we write

$$\begin{aligned} \left(i \frac{\partial}{\partial t} - \Omega_k \right) G_e(k, t-t') &= -2\pi\delta(t-t'), \\ \left(\frac{\partial^2}{\partial t^2} + k^2 c_s^2 \right) G_n(k, t-t') &= -2\pi\delta(t-t'), \end{aligned} \quad (17)$$

where we define for convenience

$$\Omega_k \equiv \frac{3}{2} \omega_e (k \lambda_e)^2 + \frac{1}{2} \frac{k^2}{k^2} \frac{\Omega_e^2}{\omega_e}.$$

Combination of (15)-(17) readily shows that

$$\begin{aligned} \delta n(k, t) &= \frac{k^2}{32\pi^2 m_i} \int_{-\infty}^{\infty} dt' \int d^3k' \frac{(k-k') \cdot k'}{k' |k-k'|} G_n(k, t-t') \\ &\times \left(\varepsilon_0(k', t') \delta \varepsilon_1^*(k-k', t') + \varepsilon_0^*(k-k', t') \delta \varepsilon_1(k', t') \right), \end{aligned} \quad (18)$$

and

$$\begin{aligned} \delta \varepsilon_1(k, t) &= -\frac{\omega_e}{4\pi n_0} \int_{-\infty}^{\infty} dt' \int d^3k' \left(\frac{k \cdot k'}{k k'} \right) G_e(k, t-t') \\ &\times \delta n(k-k', t') \varepsilon_0(k', t'). \end{aligned} \quad (19)$$

If we now write $\varepsilon_0(k, t) = \varepsilon_0(k) \exp(i\Omega_k t)$ and eliminate $\delta \varepsilon_1$ from (18) and (19), we find after some lengthy manipulations that

$$\begin{aligned}
\left(\frac{\partial^2}{\partial t^2} + k^2 c_s^2\right) \delta n(k, t) &= \frac{k^2 \omega_e}{64 \pi^2 m_i n_o} \int_{-\infty}^{\infty} dt' \delta n(k, t') \int d^3 k' |\epsilon_o(k')|^2 \\
&\times \left[\left(\frac{(k-k') \cdot k'}{k' |k-k'|} \right)^2 G_e^*(k-k', t-t') \exp[i\Omega_{k'}(t'-t)] \right. \\
&\left. + \left(\frac{(k+k') \cdot k'}{k' |k+k'|} \right)^2 G_e(k+k', t-t') \exp[i\Omega_{k'}(t-t')] \right], \quad (20)
\end{aligned}$$

where we have made use of $\epsilon_o(k) \epsilon_o^*(k') = \delta(k-k') |\epsilon_o(k)|^2$ in the derivation. Upon Fourier transformation of (20) with respect to time, we then obtain

$$\begin{aligned}
\omega^2 - k^2 c_s^2 &= -\frac{1}{4} \frac{m_e}{m_i} \omega_e^3 (k \lambda_e)^2 \int d^3 k' \frac{W_o(k')}{n_o T_e} \left[\left(\frac{(k-k') \cdot k'}{k' |k-k'|} \right)^2 \right. \\
&\times G_e^*(k-k', \omega-\omega') + \left. \left(\frac{(k+k') \cdot k'}{k' |k+k'|} \right)^2 G_e(k+k', \omega+\omega') \right] \quad (21)
\end{aligned}$$

where $W_o(k') \equiv |\epsilon_o(k')|^2 / 8\pi$ is the spectral energy density of the pump spectrum. In the further evaluation of (21), we employ a cylindrical coordinate system aligned with the ambient magnetic field in which φ (or φ') denotes the azimuthal angle. As a consequence, the dispersion equation takes the form

$$\begin{aligned}
\omega^2 - k^2 c_s^2 &= -\frac{1}{2} \frac{m_e}{m_i} \omega_e^2 (k \lambda_e)^2 \int d^3 k' \frac{W_o(k')}{n_o T_e} \\
&\times \frac{\omega_e \Omega_f(\omega, k, k')}{(\omega_\Delta + \omega_1)^2 - (\omega - 3\omega_e k k' \lambda_e^2 \cos \psi + \omega_2)^2}, \quad (22)
\end{aligned}$$

where $\omega_\Delta \equiv 3\omega_e (k\lambda_e)^2/2$, $\cos\psi \equiv [k_\parallel k'_\parallel + k_\perp k'_\perp \cos(\varphi - \varphi')] / k k'$,

$$\omega_1 \equiv \frac{1}{2} \frac{\Omega_e^2}{\omega_e} \frac{\left[k^2 (k^2 + k'^2) (k'^2 k_\perp^2 - k^2 k'_\perp'^2) - 4k^3 k'^3 k'_\parallel (k \cos\psi - k'_\parallel) \cos\psi \right]}{k^2 k'^2 [(k^2 + k'^2)^2 - 4k^2 k'^2 \cos^2\psi]}, \quad (23)$$

$$\omega_2 \equiv \frac{\Omega_e^2}{\omega_e} \frac{\left[k'_\parallel k'_\parallel (k^2 + k'^2) - k k' (k_\parallel^2 + k'_\parallel'^2) \cos\psi \right]}{(k^2 + k'^2)^2 - 4k^2 k'^2 \cos^2\psi}, \quad (24)$$

$$\Omega_f(\omega, k, k') \equiv \left[1 - \Theta \left(1 + \frac{k'^2}{k^2} \right) \right] (\omega_\Delta + \omega_1) + 2 \frac{k'}{k} \Theta \cos\psi (\omega - 3\omega_e k k' \lambda_e^2 \cos\psi + \omega_2), \quad (25)$$

and $\Theta \equiv k^4 \sin^2\psi [(k^2 + k'^2)^2 - 4k^2 k'^2 \cos^2\psi]^{-1}$.

A. The Dipole Approximation

The dipole approximation is recovered in the limit in which the wavelength of the pump tends to infinity while the wavelength spread tends to zero, and we write $W_o(k') = W_o(2\pi k'_\perp)^{-1} \delta(k'_\perp) \delta(k'_\parallel)$. Ambiguity remains, however, in the direction of the electric field of the pump, and we choose this direction to be parallel to B_o by setting $\cos\psi = k'_\parallel/k$, $\omega_1 = (k_\perp^2/k^2) \Omega_e^2/2\omega_e$, and $\omega_2 = 0$ (i.e., we take the limit $k' \rightarrow 0$ by letting $k'_\perp \rightarrow 0$ first). As a consequence, the dispersion equation in the dipole limit is of the form

$$\omega^2 - k^2 c_s^2 = \frac{1}{3} \frac{m_e}{m_i} \frac{k_\parallel^2}{k^2} \frac{W_o}{n_o T_e} \omega_e^2 \frac{\omega_\Delta \Omega_k}{\omega^2 - \Omega_k^2}. \quad (26)$$

Equation (26) can be analyzed graphically by plotting the left and right hand sides versus ω^2 . This is shown schematically in Fig. 1 in which

$$L(\omega^2) = \omega^2 - k^2 c_s^2,$$

and

$$R(\omega^2) = \frac{1}{3} \frac{m_e}{m_i} \frac{k_{\parallel}^2}{k^2} \frac{W_o}{n_o T_e} \omega_e^2 \frac{\omega_{\Delta} \Omega_k}{\omega^2 - \Omega_k^2}.$$

It is clear that the instability is purely growing (i.e., has zero real frequency), and occurs only if $R(\omega^2 = 0) < L(\omega^2 = 0)$. The threshold condition, therefore is of the form

$$\frac{W_o}{n_o T_e} > \frac{k_{\parallel}^2}{k^2} \left(3k^2 \lambda_e^2 + \frac{\Omega_e^2}{\omega_e^2} \frac{k_{\perp}^2}{k^2} \right) \left(1 + \frac{\gamma_i T_i}{T_e} \right), \quad (27)$$

where we have chosen $\gamma_e = 1$. It is important to recognize that while $(\Omega_e/\omega_e)^2$ has been assumed to be small, the effect of the magnetic field on the threshold condition can be significant when $(k\lambda_e)^2 \ll 1$ and $(k_{\perp}/k)^2 \ll 1$.

The solution to Eq. (26) takes the form

$$\omega^2 \cong - \frac{1}{3} \frac{m_e}{m_i} \frac{k_{\parallel}^2}{k^2} \frac{\omega_e^2 \omega_{\Delta} \Omega_k}{k^2 c_s^2 + \Omega_k^2} \left[\frac{W_o}{n_o T_e} - \frac{k_{\parallel}^2}{k^2} \left(3k^2 \lambda_e^2 + \frac{\Omega_e^2}{\omega_e^2} \frac{k_{\perp}^2}{k^2} \right) \left(1 + \frac{\gamma_i T_i}{T_e} \right) \right]. \quad (28)$$

As a result, we find immediately that

$$\omega^2 \cong - \frac{1}{3} \frac{m_e}{m_i} \frac{k_{\parallel}^2}{k^2} \frac{\omega_{\Delta}}{\Omega_k} \frac{W_o}{n_o T_e} \omega_e^2, \quad (29)$$

in the limit in which $m_e/m_i < 3(k\lambda_e)^2 + (\Omega_e/\omega_e)^2(k_\perp/k)^2 < W_o/n_o T_e$. In the opposite case, in which $3(k\lambda_e)^2 + (\Omega_e/\omega_e)^2(k_\perp/k)^2 < W_o/n_o T_e$ and m_e/m_i , we find that

$$\omega^2 \cong -\frac{1}{3} \frac{m_e}{m_i} \frac{k_\parallel^2}{k^2} \omega_e^2 \frac{\omega_{\Delta\Omega}^2 k}{k^2 c_s^2} \left[\frac{W_o}{n_o T_e} - \frac{k^2}{k_\parallel^2} \left(3k^2 \lambda_e^2 + \frac{\Omega_e^2}{\omega_e^2} \frac{k_\perp^2}{k^2} \right) \left(1 + \frac{\gamma_i T_i}{T_e} \right) \right],$$

so that peak growth occurs for

$$(k\lambda_e)^2 \cong \frac{1}{3} \left[\frac{k_\parallel^2}{k^2} \frac{W_o}{n_o T_e} \left(2 + \frac{\gamma_i T_i}{T_e} \right)^{-1} - \frac{\Omega_e^2}{\omega_e^2} \frac{k_\perp^2}{k^2} \right],$$

with a growth rate of

$$\omega_{\max}^2 \cong -\frac{1}{4} \left(\frac{k_\parallel^2}{k^2} \frac{W_o}{n_o T_e} \right)^2 \left(2 + \frac{\gamma_i T_i}{T_e} \right)^{-2} \omega_e^2. \quad (30)$$

B. The Case of a Monochromatic Pump

In this case we assume that the pump spectrum is aligned with the ambient magnetic field and choose $W_o(k') = W_o(2\pi k_\perp')^{-1} \delta(k_\perp') \delta(k_\parallel' - k_o)$.

Thus, we have that $\cos\psi = k_\parallel/k$, $\Theta = k_\perp^2 k^2 [(k^2 + k_o^2)^2 - 4k_\parallel^2 k_o^2]^{-1}$,

$$\omega_1 = \frac{1}{2} \frac{\Omega_e^2}{\omega_e} \Theta \left(1 + \frac{k_o^2}{k^2} \right),$$

and

$$\omega_2 = \frac{\Omega_e^2}{\omega_e} \Theta \frac{k_\parallel k_o}{k^2}.$$

It is important to recognize that the value of Θ for $k_\perp = 0$ and $k_\parallel = \pm k_o$ is dependent on the order in which the limit is taken. The source of the ambiguity is that this limit implies an interaction with

a dipole (i.e., $k \pm k' = 0$) daughter wave, and one must then specify the direction of the oscillation electric field of the daughter waves. We shall assume in the remainder of this work that the wave electric field of the daughter spectrum is parallel to the pump (and to B_0) in this limit, so that $\Theta(k_{\perp} = 0, k_{\parallel} = \pm k_0) = 0$. With this borne in mind, Eqs. (22)-(25) can be shown to reduce to the following quartic equation in

$$(\omega^2 - k^2 c_s^2)(\omega - \omega_+)(\omega - \omega_-) = \frac{1}{3} \frac{m_e}{m_i} \frac{W_0}{n_0 T_e} \omega_e^2 \omega_{\Delta} \Omega_f(\omega, k, k_0 \hat{e}_z), \quad (31)$$

where

$$\omega_{\pm} = \omega_A \left(2 \frac{k_0 k_{\parallel}}{k^2} \pm 1 \right) \pm \frac{1}{2} \frac{\Omega_e^2}{\omega_e} \frac{k_{\perp}^2}{(k^2 + k_0^2) \pm 2k_0 k_{\parallel}} \quad (32)$$

Eq. (31) has been solved numerically for a wide range of wavelengths and directions of propagation under the assumptions that $k_0 \lambda_e = 0.01$, $T_i = T_e$, and $\gamma_i = 5/3$. Some typical spectra are shown in Figs. 2 and 3, in which we plot γ/ω_e (where $\gamma = \text{Im}\omega$) versus $k\lambda_e$ for several values of θ (defined to be the angle between k and B_0) and Ω_e/ω_e . In Fig. 2, we display the typical characteristics of the spectrum for $W_0/n_0 T_e = 0.001$ and (a) $\Omega_e/\omega_e = 0$, and (b) $\Omega_e/\omega_e = 0.05$. The dotted line indicates the pump wavelength. It is clear that, as expected, the spectrum is independent of Ω_e for the case of parallel propagation, for which peak growth occurs at $k \approx k_0$ for the parameters chosen. It should be remarked, however, that this is not a general characteristic of the growth rate of parallel propagating modes, and that peak growth occurs at $k \leq k_0$ for $W_0/n_0 T_e < 0.001$ and at $k \geq k_0$

for $W_0/n_0 T_e > 0.001$. For oblique angles of propagation the growth rate vanishes in the vicinity of $k \approx k_0$, and a double peaked structure appears which describes the parametric decay and oscillating two stream instabilities. The presence of a magnetic field, typically, has a stabilizing influence on the obliquely propagating modes. In both cases shown in Fig. 2, the growth rate of the oscillating two stream instability decreases rapidly to zero with increasing θ , and the range of angles over which instability is possible decreases with increasing B_0 . The parametric decay instability is comparatively less sensitive to the magnetic field strength for the given parameters.

Additional structure appears as the pump amplitude is increased, as shown in Fig. 3 for $W_0/n_0 T_e = 0.01$. In this case, the range of θ over which instability for $k > k_0$ occurs is enlarged, and additional structure is found when $k \approx k_0$. Specifically, the growth rate does not vanish for $k \approx k_0$, and an additional peak is found when $k \approx k_0$ for small θ in the field free limit.

In order to shed light on the dependence of the growth rate on θ and Ω_e/ω_e , we plot the instability threshold, denoted by $(W_0/n_0 T_e)_{thr}$, versus $k\lambda_e$ in Fig. 4 for (a) $\Omega_e/\omega_e = 0$, and (b) $\Omega_e/\omega_e = 0.05$. It is evident that $(W_0/n_0 T_e)_{thr} \sim (k\lambda_e)^2$ for $\theta = 0^\circ$ as in the limit of a dipole pump (27); however, such behavior breaks down when $k \approx k_0$ for oblique angles of propagation. Further, it is clear that in order to excite a full angular spectrum for $k > k_0$ a threshold of $W_0/n_0 T_e \geq 0.002(0.08)$ is required for $\Omega_e/\omega_e = 0(0.05)$. This is shown in more detail in Fig. 5, in which we plot $(W_0/n_0 T_e)_{thr}$ versus Ω_e/ω_e for several values of θ and (a) $k = k_0$, and (b) $k = 2k_0$.

The dependence of the angular range of the oscillating two stream instability on β_o is shown in Fig. 6 in which we plot the maximum growth rate γ_{\max} for $k \geq k_o$ versus θ for $k_o \lambda_e = 0.01$, $\Omega_e/\omega_e = 0$, 0.05, and 0.10, (a) $W_o/n_o T_e = 0.001$, and (b) $W_o/n_o T_e = 0.01$. Evidently, when $W_o/n_o T_e = 0.001$, instability occurs only for $\theta \leq 10^\circ$ in the field-free limit, and decreases sharply in angular extent with increasing β_o . As the pump amplitude increases the angular spread of the excited spectrum also increases, as shown in the figure for $W_o/n_o T_e = 0.01$. In addition, while γ_{\max} is no longer a monotonically decreasing function of Ω_e/ω_e for all θ , substantial reductions in the growth rate are seen to occur over a wide range of angles as Ω_e/ω_e increases. The variation of γ_{\max} with Ω_e/ω_e is shown more clearly in Fig. 7.

Finally, we point out that for $W_o/n_o T_e = 0.001$ and 0.01, the parametric decay instability shows small variation with Ω_e/ω_e and θ in relation to the oscillating two stream instability. This is due to the fact that these pump levels are above thresholds for peak growth with $k < k_o$. This is demonstrated in Fig. 8 in which we plot γ_{\max} for $k < k_o$ versus Ω_e/ω_e for $\theta = 0^\circ, 20^\circ, 40^\circ$, and 60° , $k_o \lambda_e = 0.01$, and (a) $W_o/n_o T_e = 0.001$ and (b) $W_o/n_o T_e = 0.01$.

IV. SUMMARY AND DISCUSSION

We have studied the parametric decay and oscillating two stream instabilities in the presence of a weak external magnetic field, and derived a dispersion equation which can treat the case of pump spectra with small, but finite, spreads in wavelength. The result is valid for low frequencies and weak magnetic fields in which $\Omega_i \ll \omega \ll k_{\parallel} v_e$ (where Ω_i is the ion gyrofrequency) and $\omega_e^2 \gg \Omega_e^2$. Since $\omega \sim kc_s$, we must also require that $k_{\parallel}/k \gg m_e/m_i$. It should be pointed out that in (7) $\omega_{1,2}$ describe the upper and lower hybrid frequencies respectively, and that in this limit, therefore, the high frequency oscillations may also be considered as upper hybrid waves.

A few remarks are in order concerning the relationship between the directions of the ambient magnetic field, the pump spectrum, and maximum growth. For the cases considered here, in which the pump spectrum is aligned with the ambient magnetic field, the direction of maximum growth is found to be colinear with B_0 as well. While it is difficult to determine a general rule concerning this relationship, insights into the general angular spectrum of the daughter waves can be obtained by consideration of the dipole limit. In this case we let (θ_0, φ_0) and (θ, φ) denote the polar and azimuthal angles of the pump and daughter waves respectively, and find that $\omega_1 = (\Omega_e^2/2\omega_e)(\sin^2\theta - \sin^2\theta_0)$, $\omega_2 = 0$, $\cos\psi = \cos\theta \cos\theta_0 + \sin\theta \sin\theta_0 \cos(\varphi - \varphi_0)$, $\psi = \sin^2\psi$, $\Omega_k = \omega_{\Delta} + \omega_1$, and $\Omega_f = \Omega_k \cos^2\psi$. As a consequence, the instability threshold is of the form $(W_0/n_0 T_e)_{thr} = 2 \cos^{-2}\psi \Omega_k (1 + \gamma_i T_i/T_e)$. Minimizing this with respect to θ for constant (k, φ) yields

$$\tan \theta = \tan \theta_0 \cos(\varphi - \varphi_0) \left[1 - \frac{\Omega_e^2}{\omega_e^2} \left(3k^2 \lambda_e^2 + \frac{\Omega_e^2}{\omega_e^2} \cos^2 \theta_0 \right)^{-1} \right]. \quad (33)$$

Examination of (33) shows that the minimum threshold and, hence, maximum growth, for given k , is colinear with the pump wave only (1) in the field-free limit, and (2) for $\theta_0 = 0$ (i.e., when the pump and B_0 are aligned) in a magnetized plasma.

For the sake of simplicity, solutions to Eqs. (22)-(25) are restricted to the cases of dipole and monochromatic pump spectra which are in alignment with B_0 , and a substantial modification of the angular character of these instabilities is found to occur when $k^2 \lambda_e^2 \sim \Omega_e^2 / \omega_e^2$. In particular, instability thresholds tend to be enhanced, and growth rates decreased, for waves propagating at an angle with respect to B_0 . We conclude, therefore, that a small external magnetic field acts as a stabilizing influence for waves with finite k_\perp and, since $k \lambda_e \ll 1$ for many applications of practical interest, can be an important consideration in the stabilization of beam-plasma interactions even for weak field levels. Finally, because the dynamical equations for the oscillating two stream and parametric decay instabilities are the Fourier transforms of the equations which define Langmuir solitons¹³, we speculate that weak magnetic fields may act to inhibit soliton collapse in the direction transverse to B_0 .

ACKNOWLEDGMENTS

This work has been supported in part by the Office of Naval Research and in part by the National Aeronautics and Space Administration under contract W-14365. One of the authors (HPF) is an NRC/NRL Resident Research Associate.

REFERENCES

1. K. Papadopoulos, M. L. Goldstein, and R. A. Smith, *Ap. J.* 190, 175 (1974).
2. K. Papadopoulos, *Phys. Fluids* 18, 1769 (1975).
3. R. A. Smith, M. L. Goldstein, and K. Papadopoulos, *Solar Phys.* 46, 515 (1976).
4. H. Rowland and K. Papadopoulos, *Phys. Rev. Lett.* 39, 1276 (1977).
5. H. P. Freund, I. Haber, P. Palmadesso, and K. Papadopoulos, *Phys. Fluids* (submitted for publication).
6. K. Nishikawa, *J. Phys. Soc. Jap.* 24, 916 (1968).
7. K. Nishikawa, *J. Phys. Soc. Jap.* 24, 1152 (1968).
8. V. N. Tsytovich, *Nonlinear Effects in Plasma* (Plenum, New York, 1970), Chaps. V and VI.
9. P. K. Kaw, W. L. Kruer, C. S. Liu, and K. Nishikawa, in *Advances in Plasma Physics*, edited by W. B. Thompson and A. Simon (Wiley, New York, 1976), Vol. 6.
10. V. E. Zakharov, *Zh. Eksp. Teor. Fiz* 62, 1745 (1972) [*Sov. Phys. - JETP* 35, 908 (1972)].
11. W. M. Manheimer and E. Ott, *Phys. Fluids* 17, 1413 (1974).
12. G. J. Morales and Y. C. Lee, *Phys. Rev. Lett.* 35, 930 (1975).
13. W. M. Manheimer and K. Papadopoulos, *Phys. Fluids* 18, 1391 (1975).

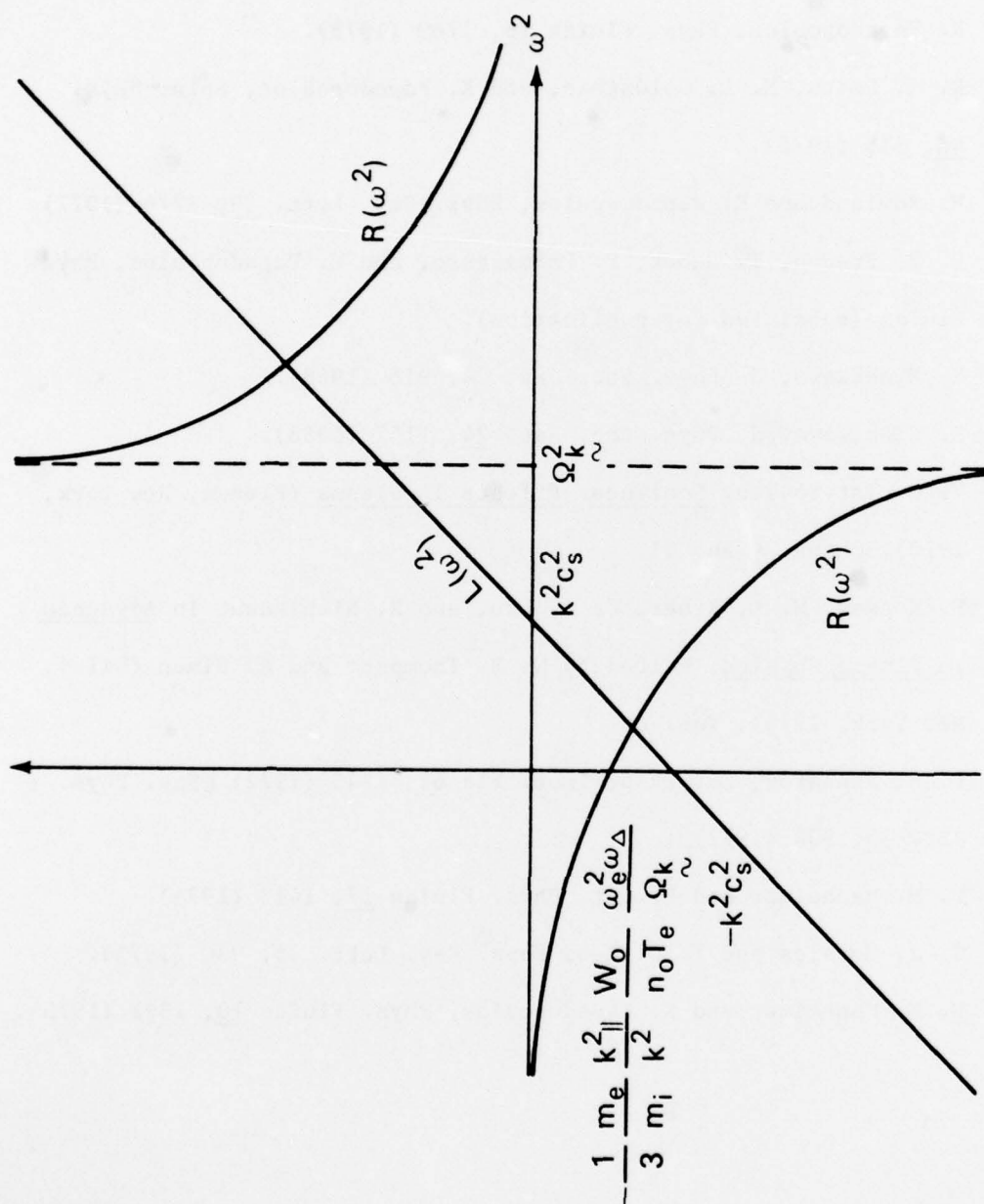


Fig. 1 — Schematic representation of graphical analysis of the dispersion equation in the dipole limit

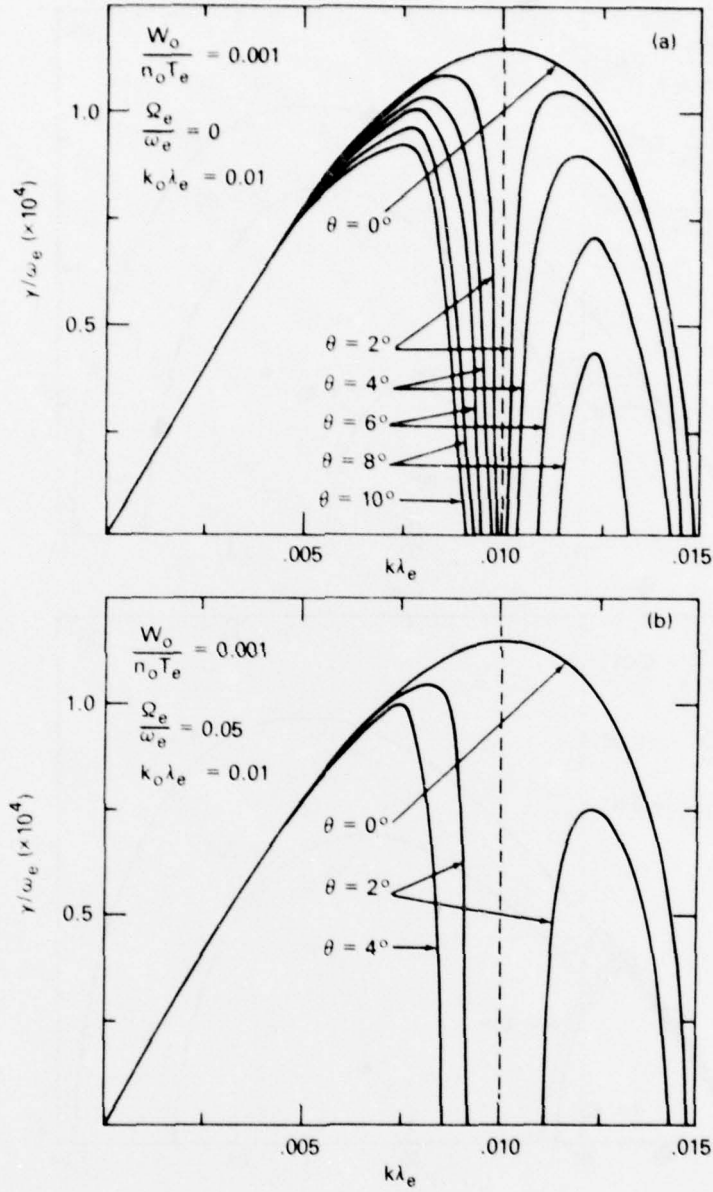


Fig. 2 — The growth rate vs. wavevector of the oscillating two stream and parametric decay instabilities for $W_0/n_0 T_e = 0.001$, $k_0 \lambda_e = 0.01$, (a) $\Omega_e/\omega_e = 0$, and (b) $\Omega_e/\omega_e = 0.05$

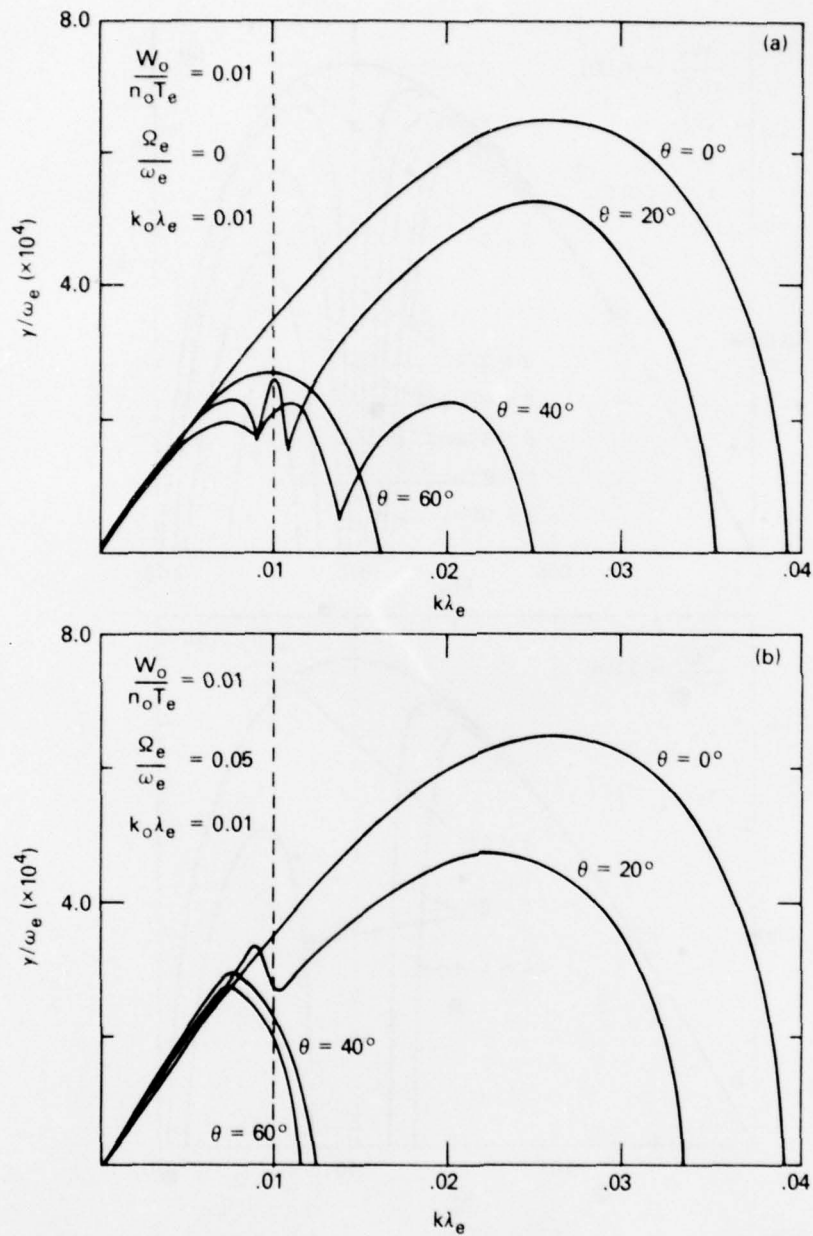


Fig. 3 — The growth rate vs. wavevector of the oscillating two stream and parametric decay instabilities for $W_0/n_0T_e = 0.01$, $k_0\lambda_e = 0.01$, (a) $\Omega_e/\omega_e = 0$, and (b) $\Omega_e/\omega_e = 0.05$

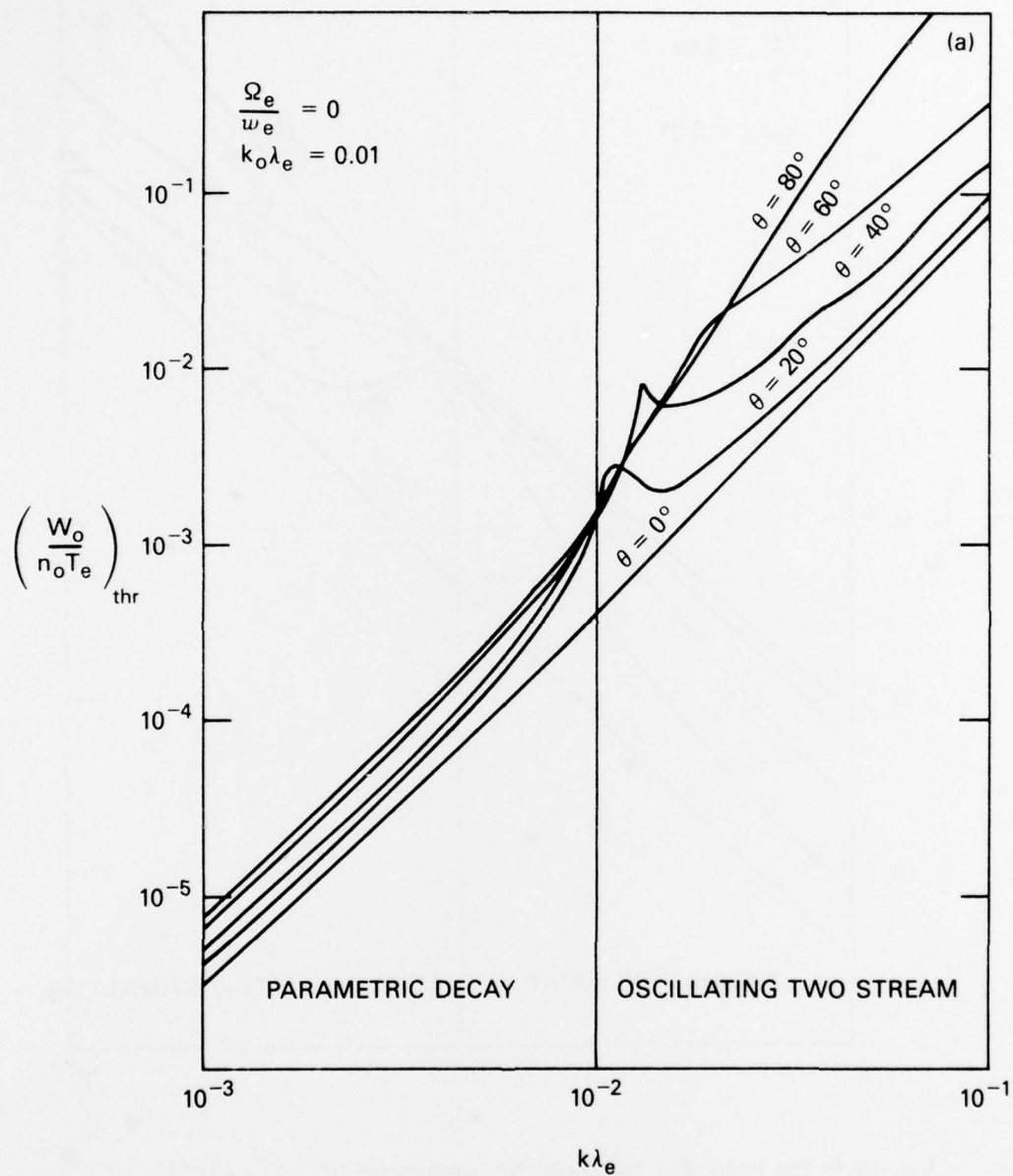


Fig. 4a — The instability thresholds vs. wavevector for $k_0 \lambda_e = 0.01$,
 (a) $\Omega_e / \omega_e = 0$, and (b) $\Omega_e / \omega_e = 0.05$

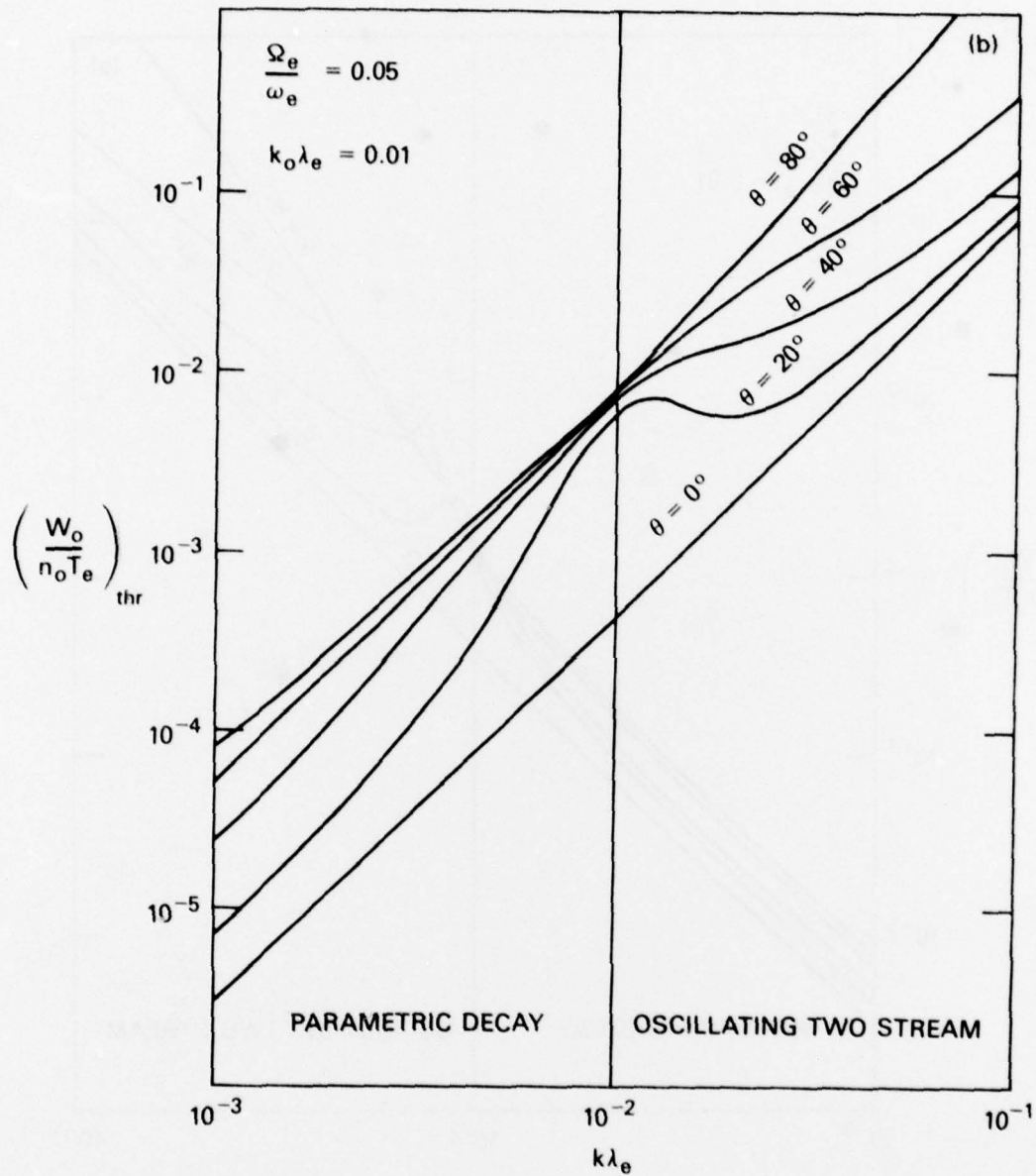


Fig. 4b — The instability thresholds vs. wavevector for $k_0 \lambda_e = 0.01$,
 (a) $\Omega_e / \omega_e = 0$, and (b) $\Omega_e / \omega_e = 0.05$

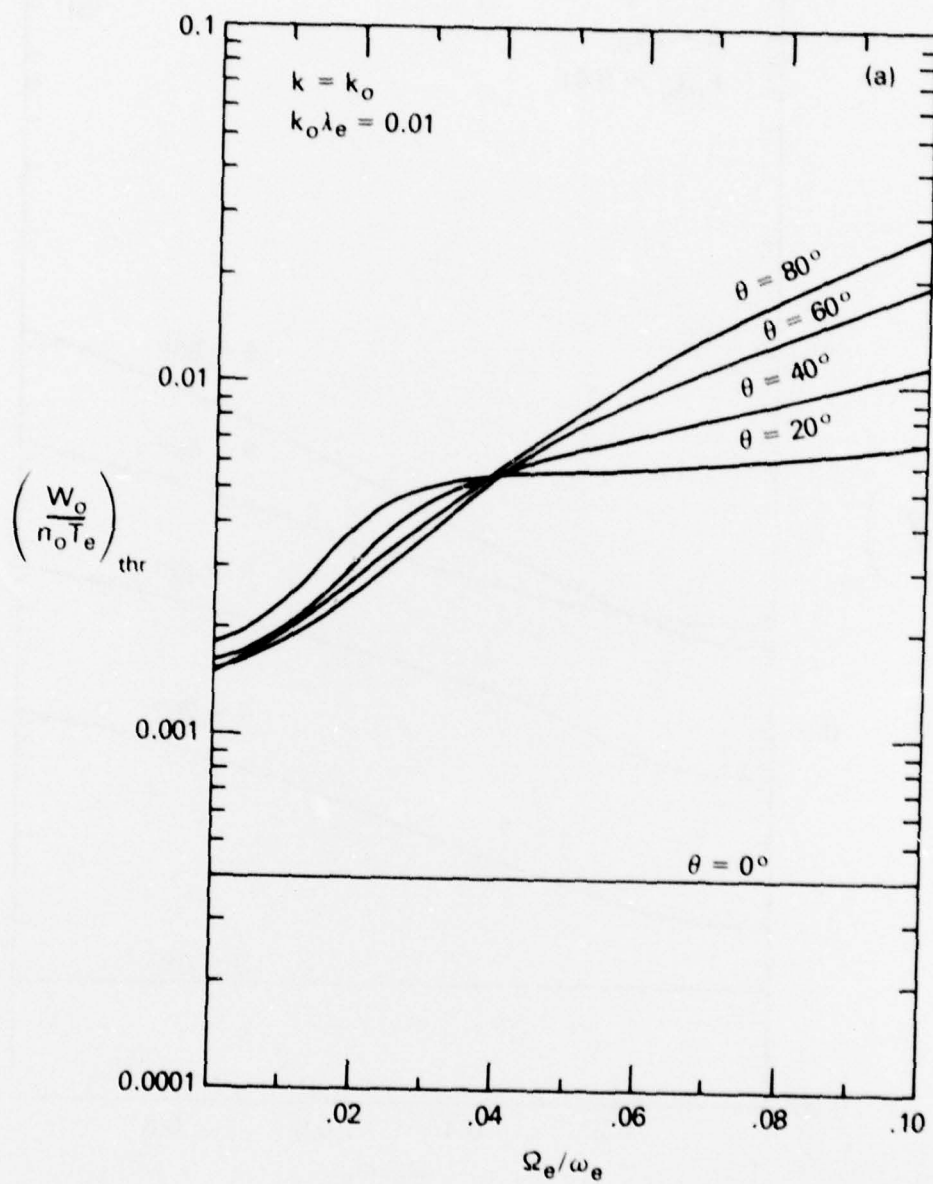


Fig. 5a — The instability thresholds vs. Ω_e/ω_e for $k_0 \lambda_e = 0.01$,
(a) $k = k_0$, and (b) $k = 2k_0$

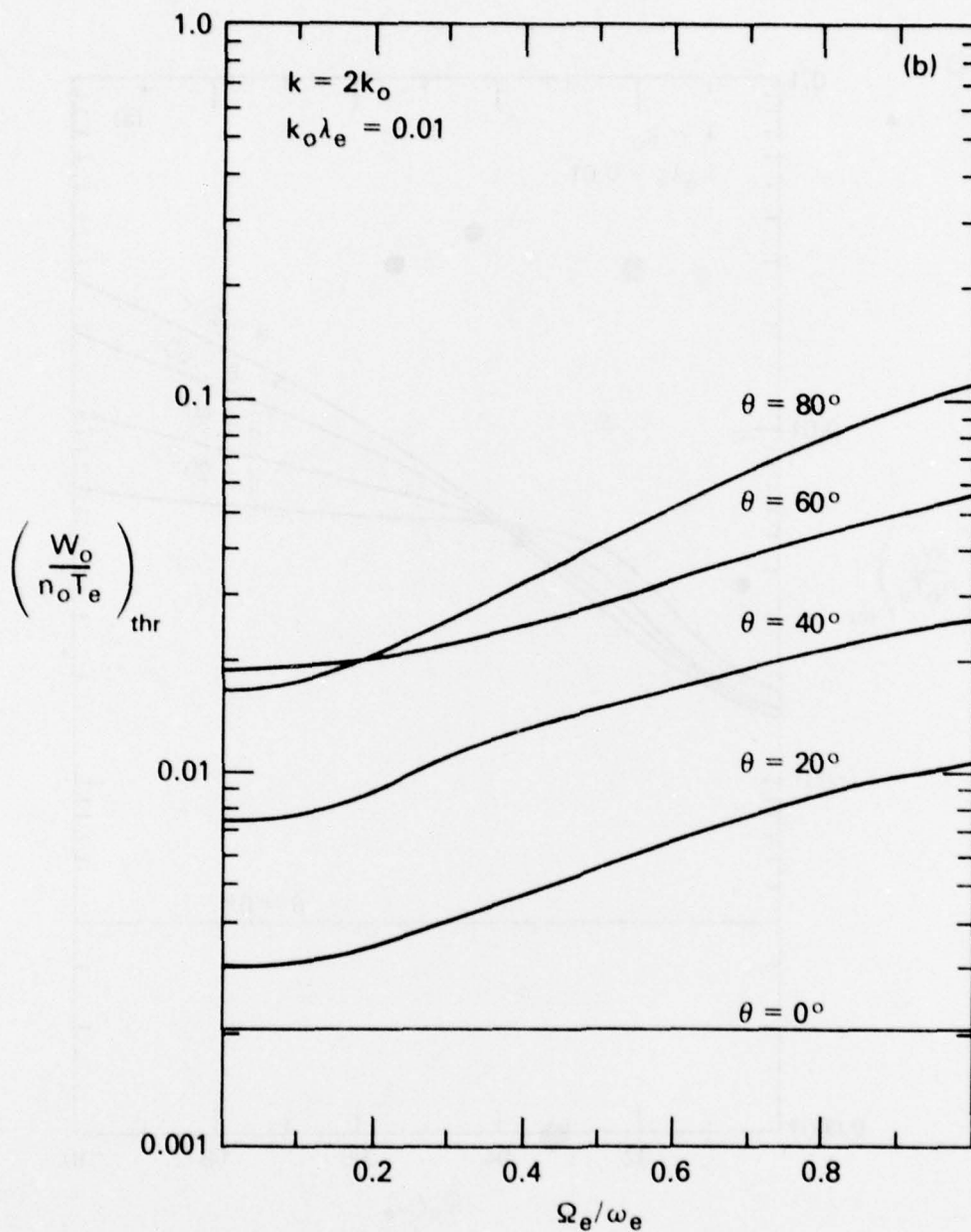


Fig. 5b — The instability thresholds vs. Ω_e/ω_e for $k_0 \lambda_e = 0.01$,
(a) $k = k_0$, and (b) $k = 2k_0$

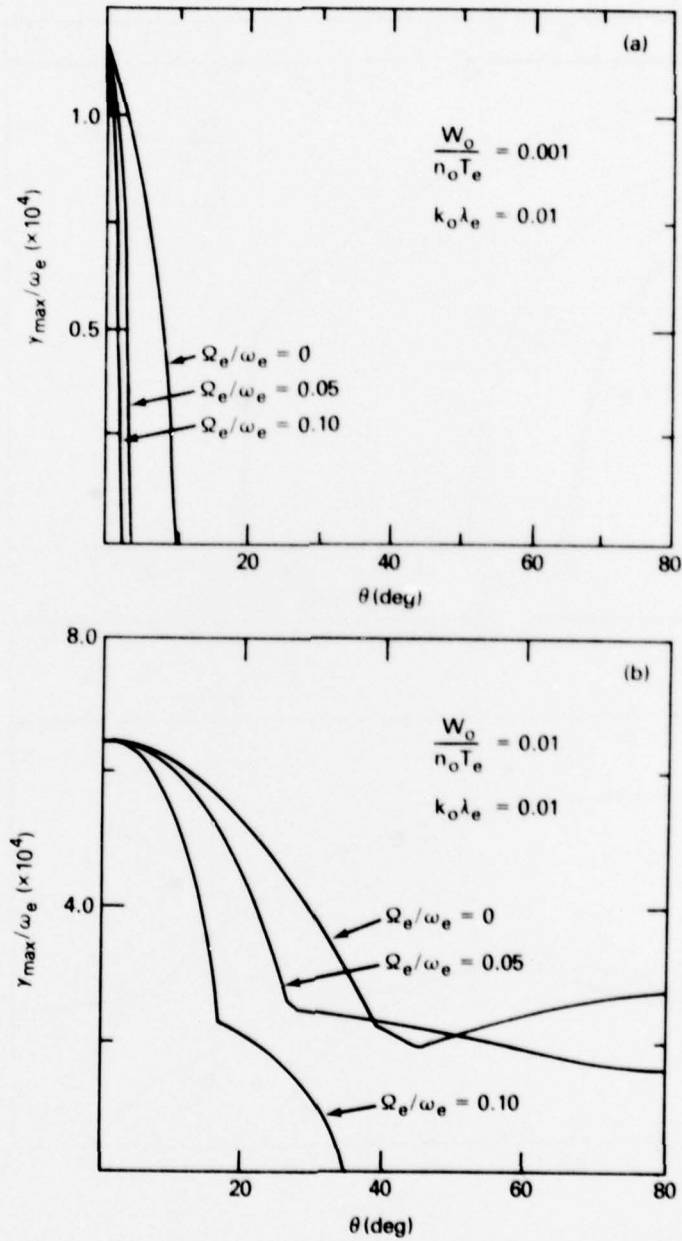


Fig. 6 — The maximum growth rate vs. θ for $k\lambda_e \geq k_0\lambda_e = 0.01$ and
(a) $W_0/n_0 T_e = 0.001$, (b) $W_0/n_0 T_e = 0.01$

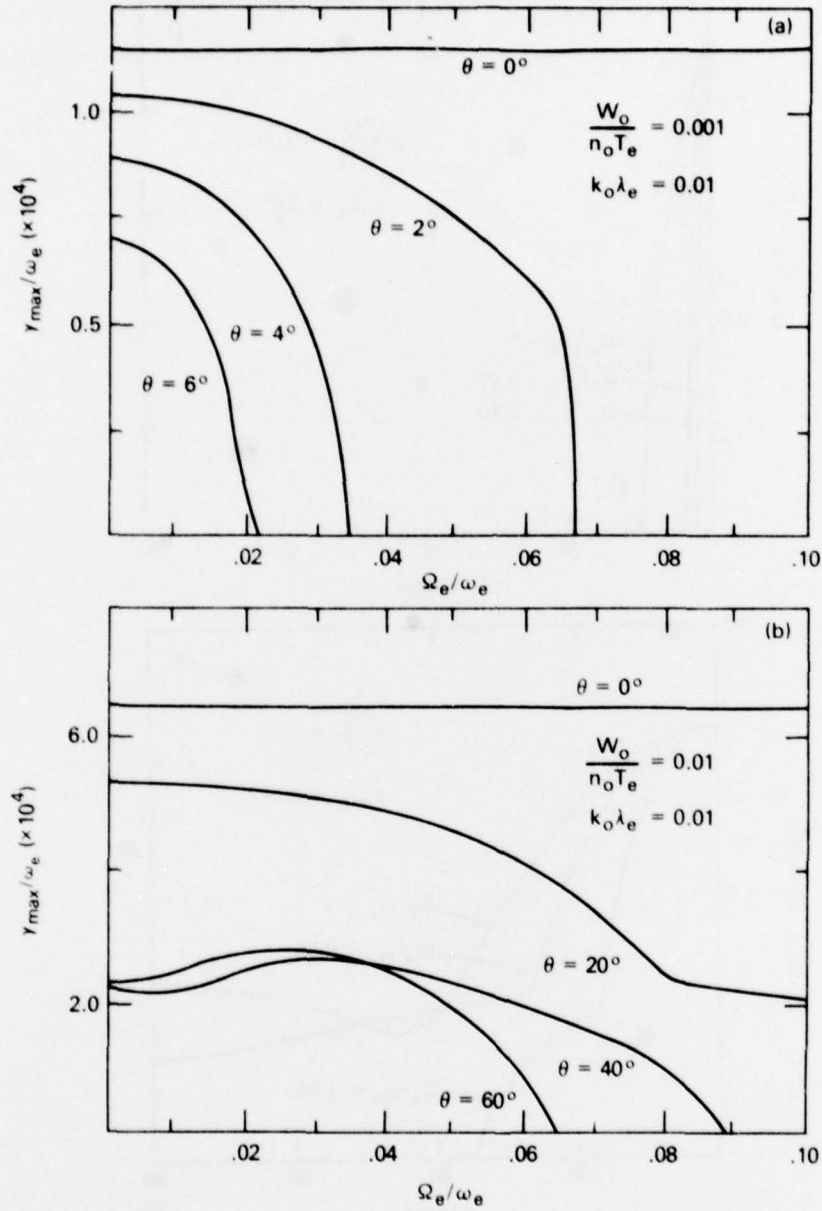


Fig. 7 — The maximum growth rate vs. Ω_e/ω_e for $k\lambda_e \geq k_0\lambda_e = 0.01$ and (a) $W_0/n_0 T_e = 0.001$, (b) $W_0/n_0 T_e = 0.01$

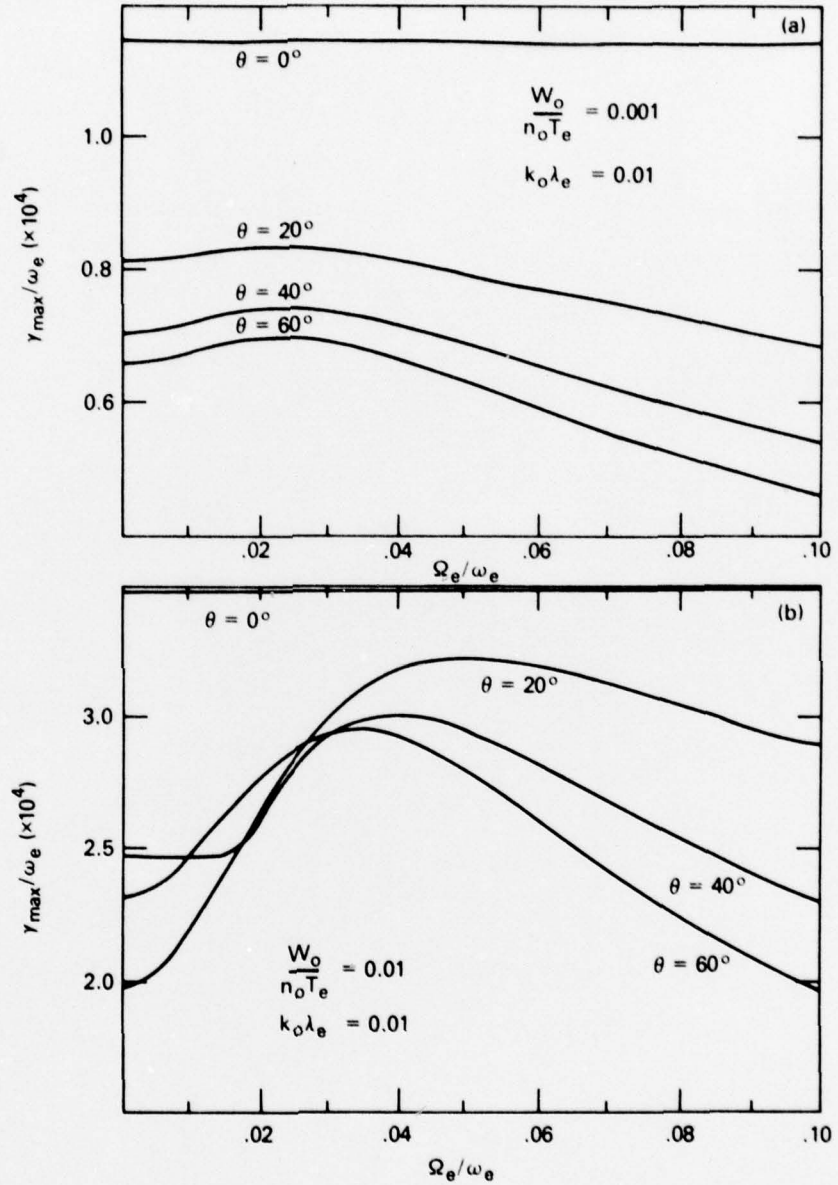


Fig. 8 — The maximum growth rate vs. Ω_e/ω_e for $k\lambda_e \leq k_0\lambda_e$ and 0.01 and (a) $W_0/n_0T_e = 0.001$, (b) $W_0/n_0T_e = 0.01$